AIAA-2002-3469

THE DESIGN OF FLIGHT STABILITY CONTROL SYSTEM AND CONSTRUCTING SIMPLE NAVIGATION SYSTEM FOR A LONG ENDURANCE AUTONOMOUS UAV

Fei-Bin Hsiao, Kuo-Wei Lin,
Meng-Tse Lee, and Wen-Ying Chang
Institute of Aeronautics and Astronautics
National Cheng Kung University, Tainan, Taiwan

Chun-Tang Chao and Chi-Fang Lin
Department of Electrical Engineering
Southern Taiwan University of Technology, Tainan, Taiwan

AIAA's 1st Technical Conference and Workshop
on Unmanned Aerospace Vehicles, Systems,
Technologies, and Operations
20-23 May 2002
Portsmouth, Virginia

1801 Alexander Bell Drive, Suite 500, Reston, VA, 20191-4344

AIAA-2002-3469

THE DESIGN OF FLIGHT STABILITY CONTROL SYSTEM AND CONSTRUCTING SIMPLE NAVIGATION SYSTEM FOR A LONG ENDURANCE AUTONOMOUS UAV

Fei-Bin Hsiao*, Kuo-Wei Lin#, Meng-Tse Lee@, and Wen-Ying Chang@

Institute of Aeronautics and Astronautics, National Cheng Kung University, Tainan, Taiwan

Chun-Tang Chao$ and Chi-Fang Lin%

Department of Electrical Engineering, Southern Taiwan University of Technology, Tainan, Taiwan

ABSTRACT

Grasping recent developments in miniature-sized computer, its peripherals, electronic sensors, and optical sensing equipment at affordable cost, the Unmanned Aerial Vehicle (UAV) with functions of long endurance and flight autonomy beyond the visual range has gradually undertaken an attractive challenge in the university. Based on this specific mission requirement and employing the existing commercial on-the-shelf products, this paper therefore focuses on the design and construction of a simple navigation and flight stability control system for the model kit size of Cessna 182 with a CCD optical payload system for taking images. Having the simplicity of construction in mind, the control laws for navigation and flight stability are designed to execute the mission along the course, through a low-cost Global Positioning System (GPS) receiver and the miniature home-designed 3-axis rate gyroscopes. With the aids of those navigation sensors, the proportional (P) control laws through the altitude holding in longitudinal direction and the other concerns of the UAV with the heading angle at less-tracking error in lateral direction.

INTRODUCTION

Nowadays the UAV system has been successfully utilized in military aspects for many decades and had a great contribution on the battlefield.[1] It is understood that the use of military UAV can reduce the casualty of pilots when executing the hostile mission such as destroying the ground targets or reconnaissance. In the most recent air campaigns, the UAV has no doubt to be able to play more important roles in the real war games. A great leap of roles and profound applications in civilian has also been made and explored. Indeed, UAV has conducted a very good function on meteorological data collection, communication relay, and optical remote sensing.

Due to attractions of UAV's applications and its technological potential, many universities in the world have concentrated on research and development of the UAVs, such as control and guidance, payload development, onboard computer system, etc. In addition, the UAV development in universities has greatly gained attention and foreseen its ample technical contributions to the education and training, in particular, on system engineering.[2] In the Remotely piloted vehicle and Microsatellite Research Laboratory (RMRL), established in early 1980s in Institute of Aeronautics and Astronautics of National Cheng Kung University, the research of UAV systems has also arisen and developed more than 15 years. [3] RMRL is one of the major research laboratories in Taiwan for UAV development. In the early days, RMRL has devoted to the design and manufacturing of different kinds of aerodynamic configurations of UAV. With the well-developed UAV, which acted as a multiple payload test bed, RMRL started to address deeper research activities on functional payload subsystem evolution since 1994. Many applications have been realized, using UAV as a platform, during last couple years, such as optical sensing, GPS navigation, and DGPS applications. The entire concept of UAV system development in RMRL can be referred to our recent review paper. [2]

In recent practical UAV applications in RMRL, the importance of beyond-visual-range (BVR) flight capability is revealed gradually as an important step in UAV development. The BVR flight capability will make aerial vehicle much more valuable for most of missions in practice, like optical remote sensing. Because of those, the real time navigation information including position and attitude is essential for BVR flight and optical payload imaging acquisition. The entire system of navigation and stability control law is designed to match up with the mission of our UAV, as shown in Figure 1. Additionally, the combination of both in hardware and software will be integrated through an onboard computer (OBC).

*Professor, Associate Fellow AIAA

$ Assistant Professor

@ Ph.D Student

M.S. Student

% Senior Student

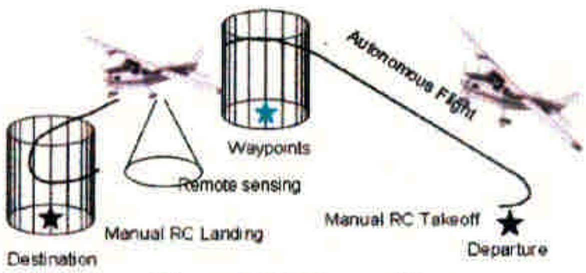

Figure 1: Mission profile

OPTICAL PAYLOAD SYSTEM

The payload system onboard the UAV is the optical observation system. The mission of the payload system is simply to catch the target image whose coordinates will be defined and stored into the OBC memories. Then, the transceiver of the system will transmit the target image to the ground station with NTSC analog signal format so that the images can be displayed on a monitor in real time.

The CCD camera is set up on a servo platform with two degrees of freedom (Figure 2). The conformation of the servo platform is similar to the gimbal type. It is designed to adjust the view of the camera on the ground target as one programmed in advance.

Figure 2: The CCD camera with a servo platform

Through GPS receiver and the home-made 3-axis gyroscope onboard, the UAV could know exactly where it is and its attitude. That information of the vehicle could be known and transferred into the OBC memory with the assigned format for coding and decoding. The driver of the servo platform will download the text file and determine the relation between the body frame coordinates of UAV and the line of sight of CCD camera (Figure. 3). After that, the servo should move and rotate the camera to pin-point to the target through the two degrees of freedom movement. The servo platform can be designed not only for swinging the compensation but also tracking the target fixed on the ground. The software architecture of the driver is based on the coordinate transformation. To improve the tracking performance and the stability of the servo platform, Kalman filtering technique is then added to further predict the body coordinates of UAV at every movement.

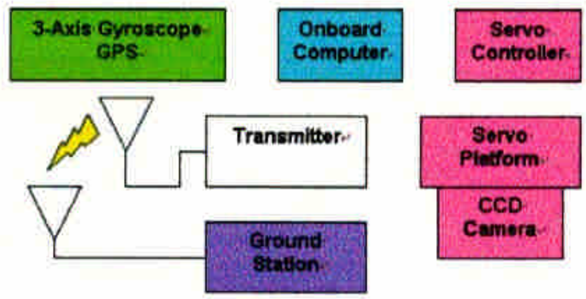

Figure. 3 The flow diagram of optical payload system

UAV FLIGHT STABILITY CONTROL

The flight parameters of the model Cessna182 are listed in Table 1. Some of the dimensionless aerodynamic coefficients are directly derived from the Jane's World Aircraft [1], the rest are calculated through DATCOM software. To simply the problem in this paper, one directly used the linear state equations for analyzing the automatic flight control system of UAV [4]. Because of the longitudinal- and lateral-directional linear state equations are decoupled, the analysis of control laws in the longitudinal and lateral direction will be performed separately.

Table 1: The flight parameter of the model Cessna182

Flight Vehicle	1/5 scale Cessna 182
Speed V_1	72.9076 (fps , 80km/hr)
Altitude h	1500 (ft)
Center of Gravity $(\overline{x}_{cg})$	0.25
Wing Area S_w	6.3249 (ft^2)
Wing Span b	6.7388 (ft)
Wing Mean Geometric Chord $\overline{C}$	0.9386 (ft)
Weight W	22.0264 (lb , 10 kg)
I_{xx}	0.3642 (slug ft^2)
I_{yy}	0.6837 (slug ft^2)
I_{zz}	0.9465 (slug ft^2)
I_{xz}	-0.0442 (slug ft^2)

In lateral direction, the purpose of control is to track a reference command of azimuth (heading angle). By using Matlab simulation program, the lateral simulation block diagram is shown in Figure 4. Two proportional gains are designed to achieve the aim of azimuth tracking. The state space equations of the lateral motion of UAV shown in Figure 4 are given by Eqation (1) and (2). After calculation shown in Figure 5~Figure 7, the gains K1=0.05 and K2=−0.02 are chosen, then the responses with the reference azimuth for a unit step input, whose final value is equal to 30 and reference yaw rate (constant input 0), are shown in Figure 5. Figure 8 and Figure 9 depict the plant inputs $\Delta\delta_a$ and $\Delta\delta_r$.

$\dot{x} = Ax + Bu$ .... (1)

$y = Cx + Du$ .... (1)

where

$x = x_{lat} = [\Delta\beta \quad \Delta p \quad \Delta r \quad \Delta\phi \quad \Delta\psi]^T$

$u = u_{lat} = \begin{Bmatrix} \Delta\delta_a \\ \Delta\delta_r \end{Bmatrix}$

$$A = \begin{bmatrix} -0.2374 & -0.0013 & -0.9926 & 0.4417 & 0 \\ -61.0914 & -15.4820 & 3.0011 & 0 & 0 \\ 14.8191 & -1.0996 & -1.1037 & 0 & 0 \\ 0 & 1.0000 & 0 & 0 & 0 \\ 0 & 0 & 1.0000 & 0 & 0 \end{bmatrix}$$

$$B = \begin{bmatrix} 0 & 0.1432 \\ 124.7371 & 8.2670 \\ -8.5858 & -17.4752 \\ 0 & 0 \\ 0 & 0 \end{bmatrix}$$

$$C = \begin{bmatrix} 0 & 0 & 1 & 0 & 0 \\ 0 & 0 & 0 & 0 & 1 \\ 0 & 0 & 0 & 1 & 0 \end{bmatrix}, \quad D = \begin{bmatrix} 0 & 0 \\ 0 & 0 \\ 0 & 0 \end{bmatrix}$$

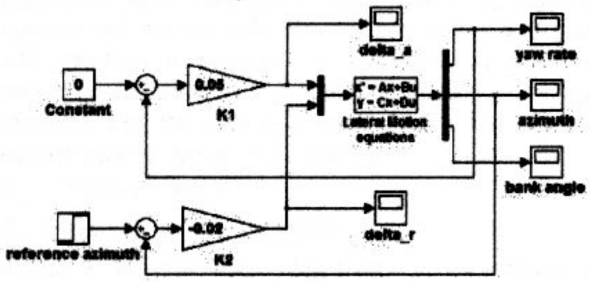

Figure 4: Simulation block diagram (lateral motion)

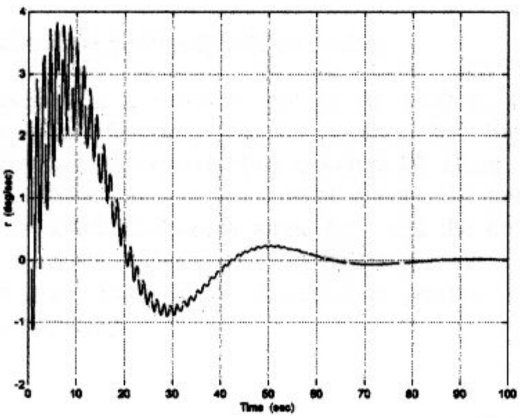

Figure 5: Yaw rate Δr versus time

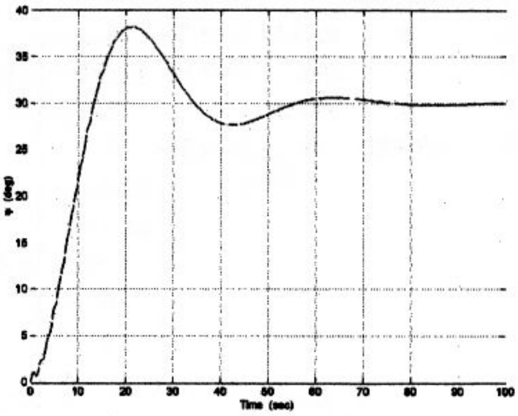

Figure 6: Azimuth $\Delta\psi$ versus time

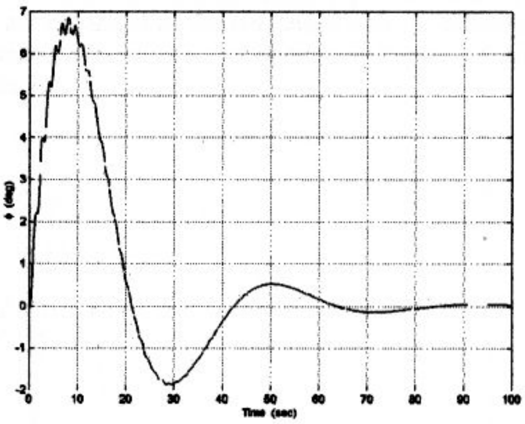

Figure 7: Bank angle $\Delta\phi$ versus time

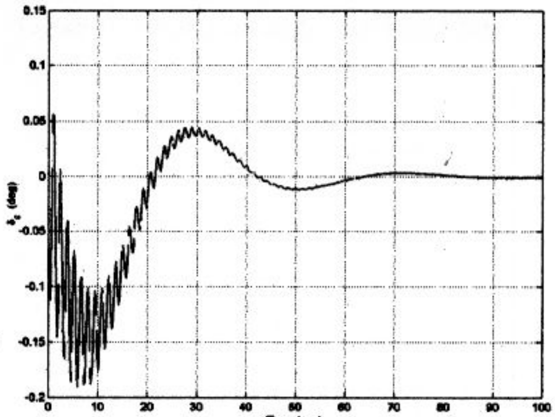

Figure 8: Deflection angle of aileron $\Delta\delta_a$ versus time

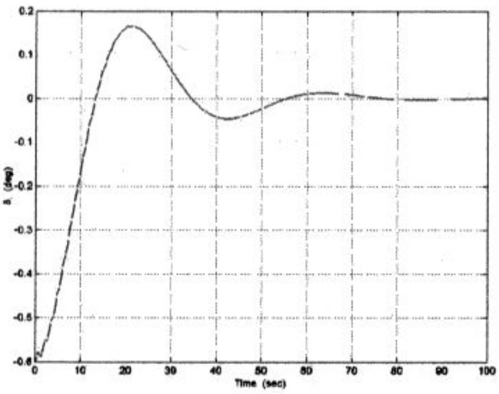

Figure 9: Deflection angle of rudder $\Delta\delta_r$ versus time

Lateral direction control surface

A positive aileron deflection means that the right hand side (back view) flap of the wing deflects upward and the left side flap deflects downward, and will produce a positive roll moment. A positive rudder deflection will produce a negative yawing moment. For the control system design, the control surface can be shown as following:

$\delta_a = -0.05 \times r$(degree)

$\delta_r = -0.015 \times (\psi_c - \psi)$(degree)

where r is yaw rate (deg/sec), ψ_c is reference azimuth command (deg) and ψ is azimuth obtain, which can be calculated by the GPS data.

Longitudinal feedback control system

For the mission that the UAV will be maintained in a constant altitude of 1500 ft, the longitudinal feedback control system for flight stability is designed according to Figure 10. There are two feedback loops in the control system, the inner loop feedback flight-path angle (γ) and the outer loop feedback altitude (h), so that there are two proportional gains to be designed to perform the altitude holding.

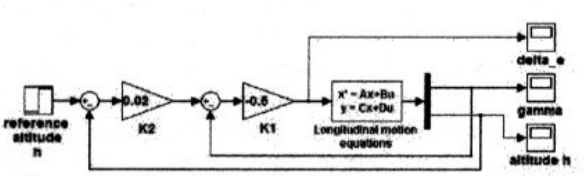

Figure 10: Simulation block diagram (longitudinal)

Longitudinal Equations of Motion:

$\dot{x} = Ax + Bu$ .... (3)

$y = Cx + Du$ .... (4)

where

$x = x_{long} = [\Delta V \quad \Delta\alpha \quad \Delta q \quad \Delta\theta \quad \Delta h]^T$

$u = u_{long} = \{\Delta\delta_e\}$

$$A = \begin{bmatrix} -0.0475 & 10.0480 & 0 & -32.2000 & 0 \\ -0.0065 & -3.5163 & 0.9726 & 0 & 0 \\ 0.0113 & -40.4848 & -5.8905 & 0 & 0 \\ 0 & 0 & 1.0000 & 0 & 0 \\ 0 & -72.9076 & 0 & 72.9076 & 0 \end{bmatrix},$$

$$B = \begin{bmatrix} -3.3493 \\ -0.3265 \\ -66.5256 \\ 0 \\ 0 \end{bmatrix}$$

$$C = \begin{bmatrix} 0 & -1 & 0 & 1 & 0 \\ 0 & 0 & 0 & 0 & 1 \end{bmatrix}, \quad D = \begin{bmatrix} 0 \\ 0 \end{bmatrix}$$

After calculation, the gains K_1 = -0.5 and K_2 = 0.02 are chosen, then the responses with the reference command *r=unit step* are shown in Figure 11 and Figure 12.

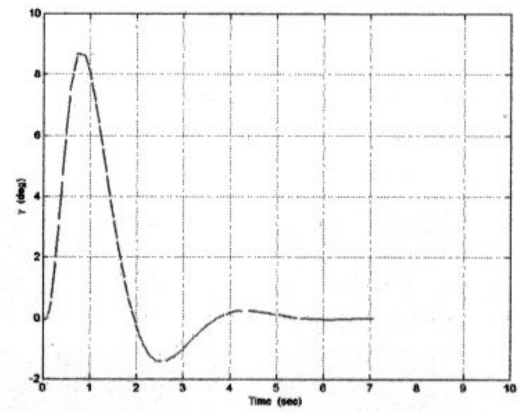

Figure 11: Flight path angle $\Delta\gamma$ versus time

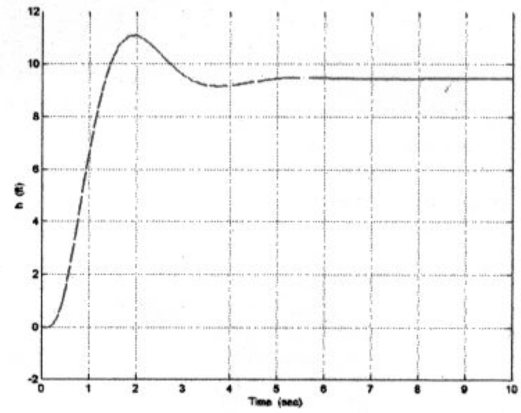

Figure 12: Altitude *h* versus time

Meanwhile, the input u denotes the deflection angle of elevator $\Delta\delta_e$, as shown in Figure 13.

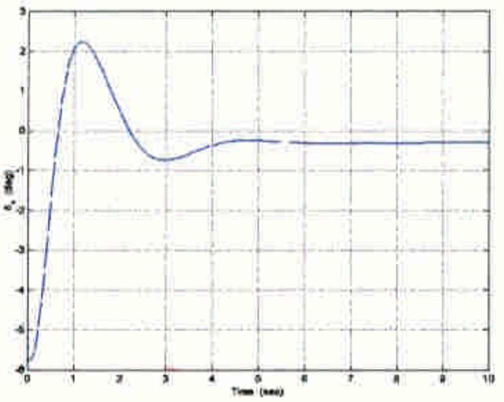

Figure 13: Deflection angle of elevator $\Delta\delta_e$ versus time

Longitudinal direction control surface

The deflection angle of elevator δ_e is positive when the elevator deflects downward with the aircraft pitch down, and

$$\delta_e = K_1 \times (K_2 \times (h_c - h) - \gamma) \times \frac{180^\circ}{\pi} \quad \text{(degree)}$$

where

K_1 = -0.5

K_2 = 0.02

h_c = reference altitude command (ft)

h = altitude of UAV feedback by altitude meter (ft)

$$\gamma = \tan^{-1}\left(\frac{\dot{h}}{\sqrt{\dot{P}_N^2 + \dot{P}_E^2}}\right) \quad \text{(rad)}$$

where $\dot{P}_N$, $\dot{P}_E$ and $\dot{h}$ are the velocities of northern, eastern and upward direction on NED frame system obtain from the GPS receiver.

NAVIGATION SYSTEM CONSTRUCTION

For the UAV to be autonomous flight beyond the visual range, more sufficient navigation information is needed. However, simply using either a single GPS or an INS seems not sufficient for UAV. Therefore, an integrated GPS/INS system is then to be used to compensate for each defect. The Remotely Piloted Vehicle & Microsatellite Lab. (RMRL) has been proceeded such a research through a single GPS engine board and Crossbow Digital Measuring Unit (DMU) in the past few years and have experienced very good result [5, 6].

However, the UAV has its congenital deficiency in volume and weight for carrying payload. The DMU is a common equipment and seems a little over-weighted for our UAV and expensive for university research. For a long-term flight UAV to execute its reconnaissance mission, the following subsystem is needed:

1. Onboard Computer System (OBC) to execute the data collection, analysis and computation, and control/monitor the UAV in flight.
2. Ground Station to monitor the real time status of UAV and uplink commands or waypoints.
3. CCD Optical Payload system to perform the air-photo mission.

The peripherals of these subsystems and payload would take most of space and weight budget in our UAV. Therefore, to develop another navigation system with small volume, less weights and low cost is the main idea to be realized in this system.

Navigation System Overview

In the construction of navigation system, the combination of the decoupled GPS and a home-made 3-axis gyroscope, used as an inertial navigation system (INS) are adopted. The uncoupled GPS and INS would perform well without any compensation with each other. The information including 3-dimensional position (longitude, latitude, and height), velocity (toward north, east and downward) and course are supplied through the GPS engine board at 1 Hz update rate. The home-made 3-axis gyroscope is designed to provide the real time Euler angles and angular rates of the UAV. Besides, an air data sensing system would be used to provide the airspeed and atmospheric pressure height. The conceptual diagram of the navigation system is shown in Figure 14.

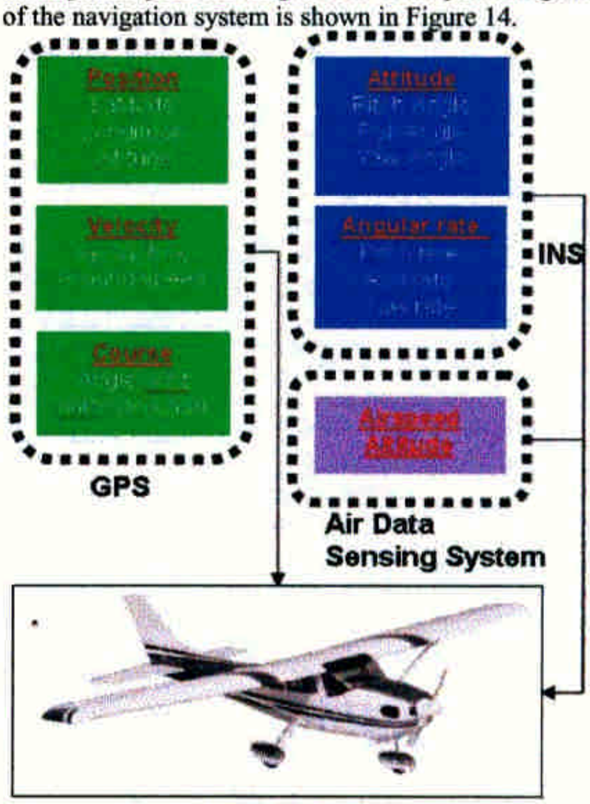

Figure 14: The conceptual navigation system diagram

GPS Receiver

The GPS receiver, GARMIN GPS-25 engine board, is used to acquire the 3D position, velocity, and course of UAV. The GARMIN GPS-25 features small size, low power consumption, low cost, and high performance. The specification is listed below in Table 2 [7].

Table 2: Performance of GARMIN GPS-25 LP

Channel	12 parallel channel
Update rate	1 second
Acquisition time	15 seconds warm (all data known) 45 seconds cold 1.5 minutes AutoLocateTM 5minutes search the sky
Accuracy 1)Position 2)Velocity	 15 meters RMS (without SA) 0.1 m/s RMS steady state (subject to Selective Availability)
Dynamics	999 knot velocity, 6g dynamics

As the deregulation of SA (Selective Availability) policy starting on May 1, 2000, the position accuracy has been proved to 7.8m (95%) horizontally and 8.6m (95%) vertically, while the update rate is still only 1 Hz. However, this accuracy and update rate are both affordable for the cruising phase of our UAV.

Home-made 3-Axis Gyroscope

To construct this 3-axis gyroscope as our inertial sensing a micro gyro ENC-03J manufactured by Murata [8] was first used in this research. ENC-03J is an angular velocity sensor that used the effect of Coriolis force, which is generated when the rotational velocity is applied to the oscillating ceramic material in the micro gyro. The output of this sensor is the analog voltage relative to its angular velocity. To verify the relationship between the analog voltage output and the angular velocity, the gyro testing equipment was designed to conduct the gyroscope's parameter identification (
Figure 15).

Figure 15: The gyroscope testing equipment

This testing equipment uses a microchip PIC16F877 to control the step motor rotating with a constant angular velocity. At the same time, the ENC 03J would have constant voltage output in relation to the specific rotation rate. Thus the characteristic curve of this gyroscope can be obtained through the linear regression analysis, as shown in Figure. 16.

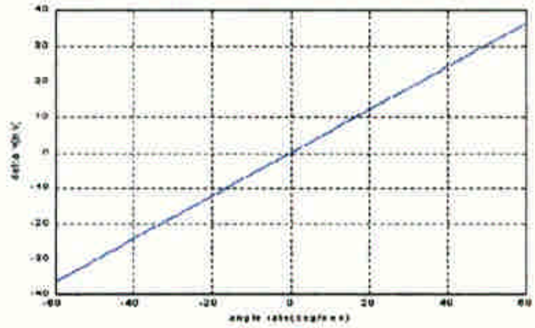

Figure. 16 Characteristic curve of ENC-03J for angular velocity versus output

This gyroscope testing equipment indeed has a great help for the construction of the home-made 3-axis gyroscope. For any other micro gyroscope adopted in the future, this equipment can be used to verify its characteristic.

In the process of calibration, it is found that ENC 03J is not suitable for use because of its instability and high noise of output. Therefore, another micro gyroscope ENV-05F-03, which is also made by Murata, is then used. The working principle of ENV-05F-03 is the same as that of ENC-03J but has better performance. The detail specification is shown in Figure 17 and Table 3.

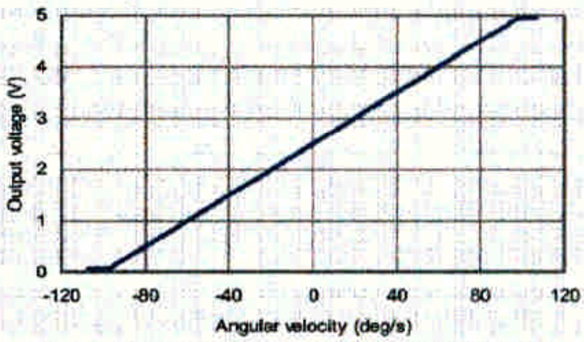

Figure 17: Characteristic curve of ENV-05F-03 gyroscope for angular velocity versus output

Table 3: The specification of ENV-05F-03

	Condition	MIN.	STD.	MAX.	Unit
Supply voltage(V_{cc})		+4.5	+5.0	+5.5	VDC
Current consumption	At V_{cc} =5.0VDC			15	mA
Max. angular velocity		-60		+60.	deg/s
Output	ω=0 at -30~80°C	2.150	2.500	2.850	VDC
Scale factor	At -10~60°C At -30~80°C	23.0 21.7	25.0 25.0	27.0 28	mV/deg/s
Temp. Coef. Scale factor	At -10~60°C At -30~80°C			5 10	%FS
Drift	At -30~80°C			9	deg/s
Linearity	In ω_{max}			0.5	%FS
Response	Phase delay: 90 deg		10		Hz
Weight				20	g
Dimension		11.5(D)×19.6(W)×23.2(H)mm			

Through Figure 17, it is known that the analog voltage output of ENV-05F-03 is linearly proportional to its angular rate. This specific curve has also been verified by the gyroscope testing equipment mentioned above.

In the design of the 3-axis gyroscope, the PIC16F877 is used as the kernel for the whole system. This is a powerful 200 nanosecond instruction execution yet easy-to-program (only 35 single word instructions) CMOS. The FLASH-based 8-bit microcontroller packs into a 40- or 44-pin package (Figure. 18). The PIC16F877 features 256 bytes of EEPROM data memory, self programming, an ICD, 8 channels of 10-bit Analog-to-Digital (A/D) converter, 2 additional timers, 2 capture/compare/PWM functions. The synchronous serial port can be configured as either 3-wire Serial Peripheral Interface (SPI™) or the 2-wire Inter-Integrated Circuit (I2C™) bus and a Universal Asynchronous Receiver Transmitter (USART). All of these features make it ideal for more advanced level A/D applications in automotive, industrial, appliances and consumer applications [9].

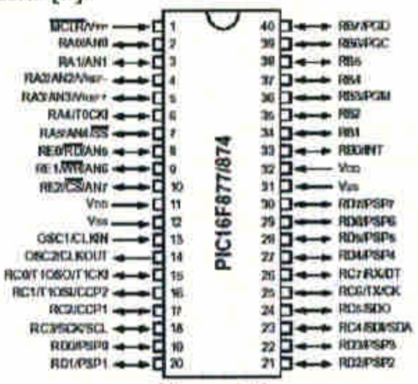

Figure. 18

When a angular rate is sensed by the ENV-05F-03 gyroscope, the related voltage would transfer to the microchip through its I/O port. The A/D converter of PIC16F877 would turn the analog signal to digital with 8-bit resolution. And then, the digital signal would be transformed to the value of related angular rate (Figure 19).

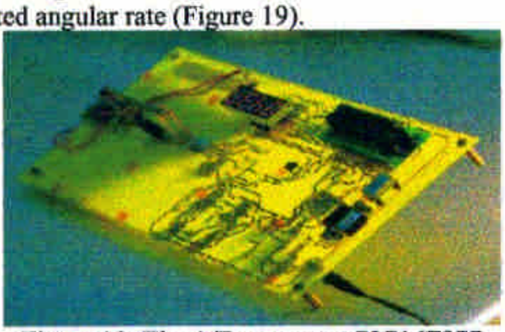

Figure 19: The A/D converter PIC16F877

Air Data Sensing System

The air data sensing system acquires the pressure altitude and airspeed information. For the use of the pressure altitude sensor (Figure 20), the R/C altitude holding module is modified and just wired to the signal line from the amplifier to the A/D board of UAV Onboard Computer. Since there is no pressure data about the absolute pressure sensor, the calibration of the pressure sensor is necessary for practical applications. The calibration was done by mountain climbing from the IAA building, about sea level, to Yushan National park, about 3,000m in height from sea level. The relationship between the output voltage and the actual height is shown in Figure 21. The linearity is surely obtained in corresponding to a fitting line.

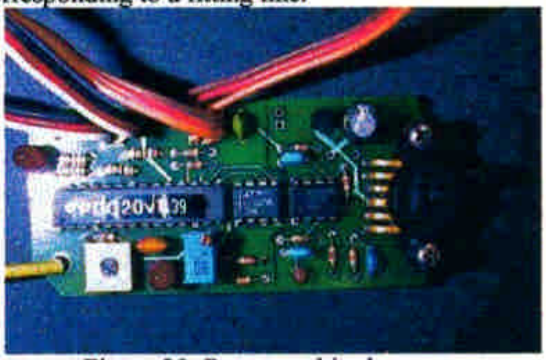

Figure 20: Pressure altitudesensor

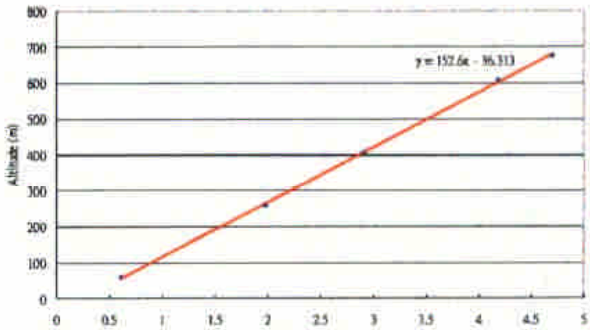

Figure 21: Altitude vs. sensor voltage output

Another air data is the airspeed sensor (Figure 22), which was also modified from a commercial R/C holding module. Similarly, the signal line was wired from the amplifier to the A/D board on OBC. The calibration was done in an open type wind tunnel. The calibration range is from 0 to 30m/s. The result is shown in Figure 23 with a fitting curve of a 4^{th}-order polynomial line.

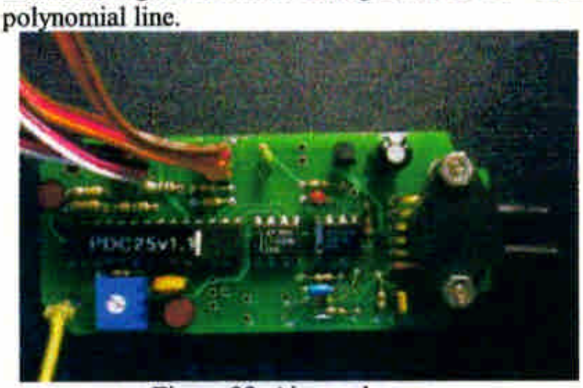

Figure 22: Airspeed sensor

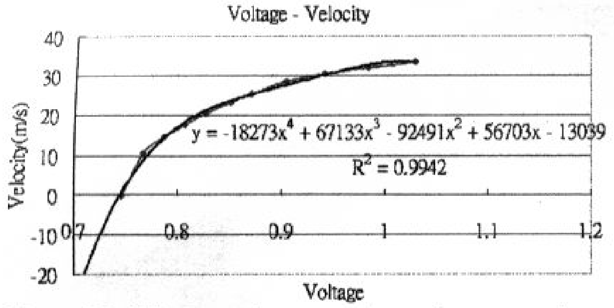

Figure 23: Wing speed versus airspeed sensor voltage output

RESULTS AND DISCUSSION

Once the whole UAV system is integrated, which including the aircraft itself, payload system, control/navigation system, and the ground station system, the model kit UAV is ready to start the ground and flight tests. Since considering the acute dynamic motion of UAV, the instability of equipment onboard, the electromagnetic interference (EMI) effect, and the piston engine vibration, the tests of all the equipment are necessary in static and dynamic environment. Before the flight test proceeds, the ground test is first proceeded to reduce some possible risks to verify the flight stability of the whole system. Some important results are discussed as following:

1. Test of home-made 3-axis gyroscope:
   This system would be placed on the static level flat plate for a long time to check if the angle and angular rate output from the 3-axis are zero or not. The drift effect is also our concern in the run test. After that, the gyroscope will be rotated to certain angles to make sure whether the angle output is exactly right.
2. Ground vehicle moving test:
   The GPS receiver and air data sensing system will be put on the ground vehicle with the onboard computer to collect the track of the vehicle and test the stability of the equipments.
3. The tracking function of the optical sensing system will be tested through the input information from 3-axis gyroscope.

After the ground testing, all the system will be installed on the UAV to perform the flight test. One torque compensation gyroscope, GWS PG-01 [10] is used on UAV to sense the yaw rate and then output the PWM signal to control the aileron motion for the purpose of maintaining the UAV at desired attitude. Both attitude data from 3-axis gyroscope and GPS information will be transferred to the onboard computer for modification of the stability control law in the future. The real flight test for the mission of autonomous waypoint flight is undertaking on campus and the first phase flight data will be provided and analyzed to be compared with the control design.

CONCLUSION

This paper presents the recent results of our new UAV system with GPS incorporated with a home-made 3-axis gyroscope for carrying out the beyond-visual-range flight. A self-made navigation system is developed and demonstrated to be economic equipment for flight stability and navigation in the current study. Before finishing the full-developed navigation system, a simple flight stability and control with the control gains in lateral and longitudinal directions are also analyzed using the existing software tools and shall be proved by real flight tests.

From the simulation results of the stability control system, it is known that there exists certain inherent limitation for simply using the proportional control. The dynamic performance of UAV should be further promoted. Thus, more real-time navigation information is indeed necessary to be given during the flight. After completing the P-control flight test, the PID control will then be further conducted to improve the performance of the UAV in autonomous flight.

ACKNOWLEDGEMENT

This work is supported by the National Science Council, R.O.C., under the Contract no. NSC 90-2212-E-006-141.

REFERENCE

[1] Jane's Unmanned Aerial Vehicle, 2001.
[2] Hsiao, F. B. and Lee, M.T., "The Development of Unmanned Aerial Vehicle in RMRL/NCKU," 4th Pacific International Conference on Aerospace Science and Technology, Kaohsiung, Taiwan, May 21-23, 2001.
[3] Hsiao, F.B. and Lee, M.T., "System Engineering and Practice in Aircraft Design for Aerospace Education," UNESCO 4th Annual Conference on Engineering Education, Bangkok, Thailand, 7-10 February 2001.
[4] Nelson, R. C., "Flight stability and automatic control" 2nd edition, McGraw-Hill Co.,1998
[5] Juang, J. W., "Development of Navigation Payload System for Unmanned Aerial Vehicle", Master thesis, National Cheng Kung University, June, 1999.
[6] Hsiao F.B., Fang K.J., "Real Time Attitude Determination of Remotely Piloted Vehicle Using GPS Doppler Velocity Measurements", Transactions of Aerospace Science and Technology of ROC, Sep., 2000.
[7] Garmin International Inc., http://www.garmin.com
[8] Murata Electronics North America, Inc. http://www.murata.com/
[9] Microchip Technology Inc., http://www.microchip.com/
[10] Grand Wing Servo-Tech. Co., Ltd. http://www.grandwing.com.tw/